The two-way memory effect in a 50 at.% Ti-40 at.% Ni-10 at.% Cu alloy

1995 J. Phys.: Condens. Matter 7 3709

(http://iopscience.iop.org/0953-8984/7/19/005)

J. Phys.: Condens. Matter 7 (1995) 3709–3720. Printed in the UK

The two-way memory effect in a 50 at.% Ti–40 at.% Ni–10 at.% Cu alloy

G Airoldi†, T Ranucci‡, G Riva§ and A Sciacca‡

† Dipartimento di Fisica, Università di Milano, via Celoria 16, 20133 Milano, Italy
‡ Istituto per la Tecnologia dei Materiali Metallici non Tradizionali, Consiglio Nazionale delle Ricerche, via Bassini 15, 20133 Milano, Italy
§ Istituto Nazionale per la Fisica della Materia, Unità di Milano Università, via Celoria 16, 20133 Milano, Italy

Received 13 December 1994

Abstract. The two-way memory training across the B2 ↔ B19 transformation of a 50 at.% Ti–40 at.% Ni–10 at.% Cu alloy has been investigated here following both the strain and the electrical resistance change.

Training loops of the form

(P → M transformation → strain → shape recovery on reverse transformation)

under applied stress levels of 51, 70.1, 89.2 and 108.3 MPa have been examined. The chief aim of the paper has been both to detect the electrical resistance change across the B2 ↔ B19 transformation, which is linearly related to the strain, and to discuss the different contributions related to the electric transport properties. The results found here provide sound support for selecting the electrical resistance as a state control variable in a two-way memory effect device.

1. Introduction

It is known that the two-way memory effect (TWME) in shape memory alloys is imprinted by means of a repetitive procedure called *training*. Defining P as the parent phase and M as the martensitic phase, the simplest training method consists of several loops as follows:

(P → M transformation → strain → shape recovery on reverse transformation).

The application of a constant stress during the above-described training procedure improves the efficiency of training, allowing one to obtain the same TWME strain by performing a lower number of training cycles [1–3]. On the atomic scale, training creates a pattern of line defects which stabilizes a preferred growth of variants, during P→M thermally induced transformations performed after training; a macroscopic reversible shape change can as a consequence be settled [4, 5].

The TWME has been thoroughly investigated for Ti–Ni shape memory alloys, involving the training of monoclinic B19′ martensite variants, by considering also the effect of the martensitic rhombohedral R-phase, intermediate between the parent body-centred cubic B2 phase and the martensite B19′ [2, 3]. Literature data on TWME in the Ti–Ni–Cu alloys are on the contrary lacking.

In the 50 at.% Ti–40 at.% Ni–10 at.% Cu alloy, two thermoelastic martensitic transformations are present: from parent B2 to orthorhombic B19 martensite and from

0953-8984/95/193709+12$19.50

B19 to monoclinic B19′ martensite. B2 ↔ B19 transformation is characterized by a narrow temperature hysteresis cycle [6–8] and, in the stress-induced martensite region, by a narrow stress hysteresis cycle [9]. The 50 at.% Ti–40 at.% Ni–10 at.% Cu alloy appears an ideal system to investigate the impact of B19 variants in the TWME. The effects of training confined to B2 ↔ B19 transformation in a 50 at.% Ti–40 at.% Ni–10 at.% Cu shape memory alloy are here investigated focusing the attention on the electrical resistance change connected with the set-up of TWME.

2. Experimental details

Commercial wires (diameter, 1 mm) of 50 at.% Ti–40 at.% Ni–10 at.% Cu, kindly supplied by Furukawa Electric Co., have been examined. Specimens 145 mm in length have been heat treated by aging at 723 K (3.6 ks) plus water quenching (WQ) at room temperature, followed by a solution treatment at 1123 K (3.6 ks) plus WQ.

Differential scanning calorimetry (DSC) measurements in the temperature (T) range 220–370 K were performed with a Perkin–Elmer DSC7 PClab instrument, at 0.017 K s^{-1} scan rate, to check the B2 ↔ B19 and B19 ↔ B19′ transformation temperature ranges. Electrical resistance (ER) versus T measurements in the range 80–370 K were carried out using a conventional four-terminal DC method with a digital micro-ohmmeter ESI 1701B.

Mechanical tests were carried out with a 1455 Zwick testing machine (cell load, 200 N), equipped with a thermostatic chamber operating between 300 and 356 K; the strain ε was detected with a Zwick extensometer (gauge length, 10 mm; range, ±0.5 mm). The specimen temperature was detected with three T-type thermocouples, spot welded one inside the gauge region, and the others outside the electrical connectors region. Training to imprint the TWME was achieved by ten thermal cycles inside the range 300–365 K, involving just the B2 ↔ B19 phase transformation, at different constant tensile stress levels (51, 70.1, 89.2, and 108.3 MPa) applied, at the start, in the parent phase.

3. Results

3.1. Characterization

Typical DSC scans are shown in figure 1. In figure 1, curve a, the sharp peak of the B2 → B19 transition appears on cooling, followed by the broad smooth signal of B19 → B19′ martensite-to-martensite transformation, for which a small heat of transformation is expected as shown in [7, 8]; the reverse sequence is found on heating. In figure 1, curve b, the partial cycle subsequent to the full cycle shown above, related to the B2 ↔ B19 transformation, is plotted.

Table 1. B2 ↔ B19 transformation temperatures detected by DSC and ER measurements.

	M_s (K)	M_f (K)	A_s (K)	A_f (K)
DSC	323	314.7	323.8	332.5
ER	324.8	314.7	318	335.8

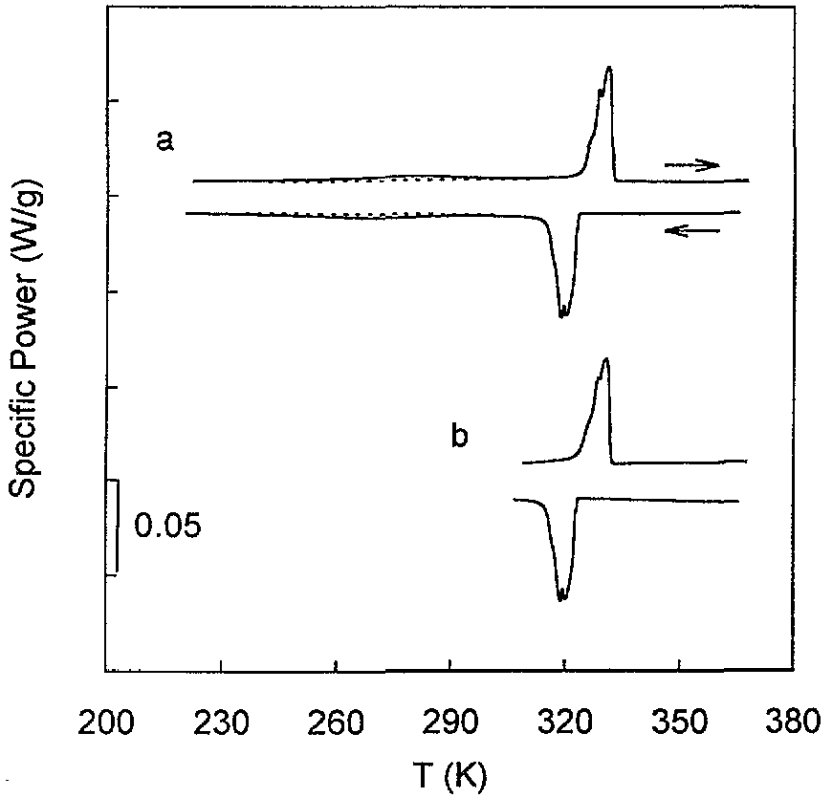

Figure 1. DSC scans showing (a) the double step of the two transformations B2 ↔ B19 ↔ B19′ and (b) a partial cycle involving only the B2 ↔ B19 transformation.

In figure 2, ER versus T down to 80 K is plotted; the slight modification at $T \simeq 320$ K corresponds to the B2 ↔ B19 transformation; a large ER change in a wide range of temperatures occurs on the contrary during the B19 ↔ B19′ transition. In the inset a magnification of the range 300–365 K, selected for the TWME training, related to the B2 ↔ B19 transformation, is given. The transformation temperatures related to the B2 ↔ B19 transition, detected by DSC and ER measurements, are shown in table 1.

From both DSC and ER measurements we can see the narrow hysteresis cycle of the B2 ↔ B19 transformation and its separation on the temperature scale from the B19 ↔ B19′ transformation, in agreement with literature data [6–8].

3.2. Training and two-way memory effect; variation in the electrical transport properties

In figure 3 the ε versus T curves, related to the training at 70.1 MPa, are plotted; curve a corresponds to a thermal cycle before training (in the stress-free condition), curves b and c are related to the first and tenth training cycles, respectively (the large elongation (contraction) corresponds to selected variants growth (shrinkage) during B2 → B19 (B19 → B2) transformation); curve d corresponds to the thermal cycle after training, in the stress-free condition (ε_{tw} is the imprinted TWME). The plastic strain ε_p, detected in the B2 phase after the first and tenth training cycles, is shown. The elastic strain ε_{el}, settled on loading in the B2 phase at the start of training, is also shown.

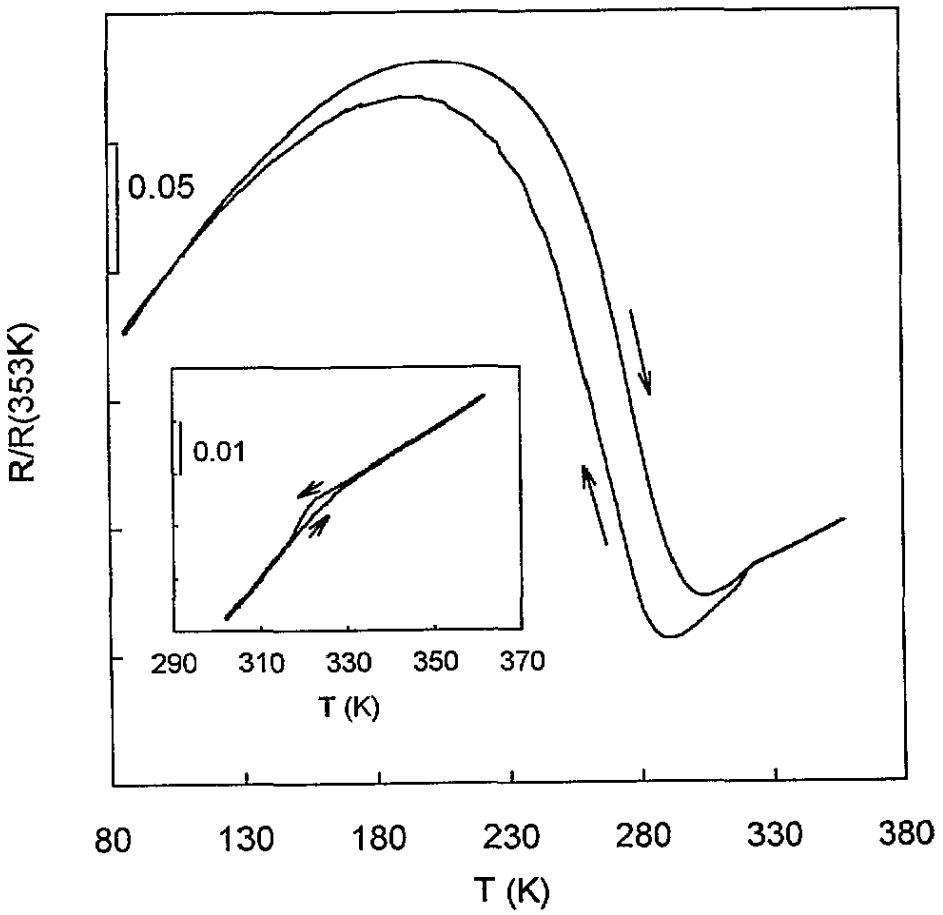

Figure 2. $R/R(353\ \mathrm{K})$ versus T curves showing the double step of the two transformations B2 ↔ B19 ↔ B19′ and (inset) a partial cycle limited to the B2 ↔ B19 transformation.

In figure 4 the relative ER variation $\Delta R/R_0$ versus T, detected during the same tests related to the ε versus T plots in figure 3, is given. $\Delta R = R - R_0$, where R_0 is the ER at the start of training in the stress-free B2 phase (at $T = 350$ K). There is much evidence that the large ER variation, which arises as a consequence of training, occurs in the temperature range of the B2 ↔ B19 transformation.

The two-way (reversible) strain ε_{tw} and the plastic strain ε_p stored as a consequence of the ten training cycles are given in figure 5 as functions of the training stress. ε_{tw} is nearly constant at stresses higher than 70.1 MPa; on the contrary, ε_p grows steadily with increasing applied training stress.

The plastic strain increases with increasing number of training cycles, as can be seen in figure 6, for all the stresses investigated. While the plastic strain increases almost linearly with increasing number of training cycles at 51 and 70.1 MPa applied stresses, at higher stresses the steepest increase is found during the first three to four training cycles.

In figure 7, $\Delta R/R_0$ for each training cycle at $T = 350$ K in the B2 phase is plotted as a function of the plastic strain; except for the highest stress level (108.3 MPa), a linear relationship is found, with slopes of 2.64 at 51 MPa, 2.51 at 70.1 MPa, and 2.62 at 89.2 MPa.

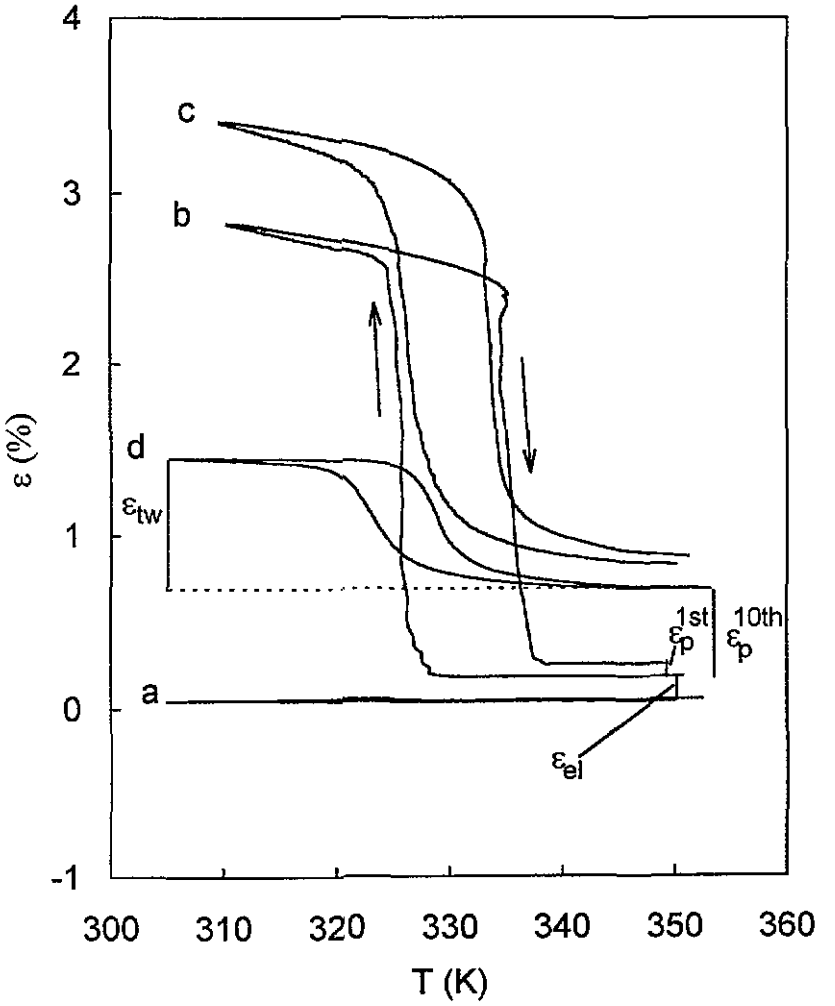

Figure 3. ε versus T during the thermal cycle: (a) before training; (b) at a stress of 70.1 MPa during the first training cycle; (c) at a stress of 70.1 MPa during the tenth training cycle; (d) after training.

Resetting R_0 at the start (finish) of the transition region on cooling (heating), $\Delta R/R_0$ versus ε curves across the transition region during the first (curve a) and tenth (curve b) training cycles at 70.1 MPa, and during the thermal cycles (curve c) after training, corresponding to the TWME, are given in figure 8. The curves related to the B2 → B19 transition (elongation) and to the reverse B19 → B2 (contraction) become almost superimposed with training. A similar behaviour, although confined to a smaller elongation, is found during the TWME.

Quite similar results have been obtained under the other training stresses investigated here, as shown in figure 9, where $\Delta R/R_0$ versus ε during the tenth training cycle, for each training stress, is plotted. The trend found is quite similar for all the training stresses investigated except at the lowest stress level (51 MPa), where a greater deviation from linearity is found during the reverse transformation.

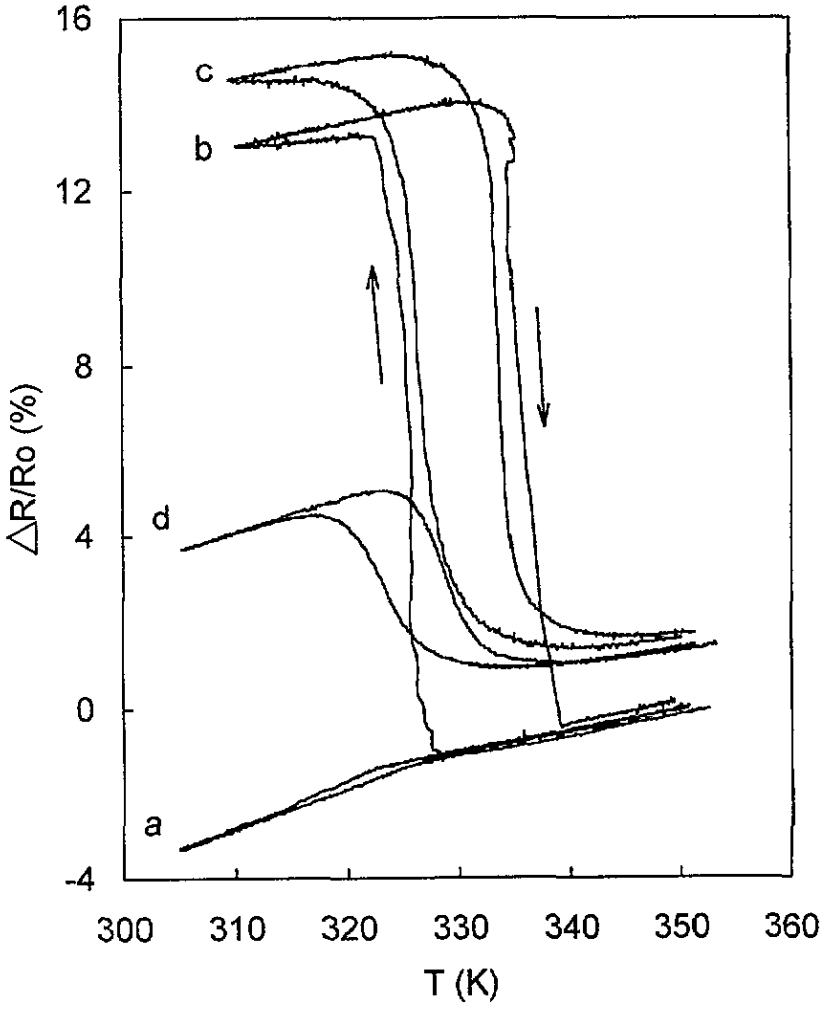

Figure 4. $\Delta R/R_0$ versus T curves related to the ε versus T curves shown in figure 3.

4. Discussion

The ε_{tw}-values obtained by the training of B19 orthorhombic martensite variants, given in figure 5, has already reached a value of about 0.8% at 70.1 MPa; this value looks low, when contrasted with literature data concerning the training of monoclinic B19′ variants in Ti–Ni [3]. Data related to the training of orthorhombic martensite are, however, lacking in the literature and a comparison cannot be made. However, recent ε_{tw} results on a 50 at.% Ti–40 at.% Ni–10 at.% Cu alloy, obtained by a different training method, confirm the value found here, supporting an upper limit of about 1% for ε_{tw} related to the B2 ↔ B19 transition [10].

The chief aim of the present investigation was the analysis of the electrical transport properties across the transformation range either during or after training to imprint the TWME, in the case where a low ER change ascribed to the thermally induced phase transition is present. The B2 ↔ B19 transformation in 50 at.% Ti–40 at.% Ni–10 at.% Cu is an ideal

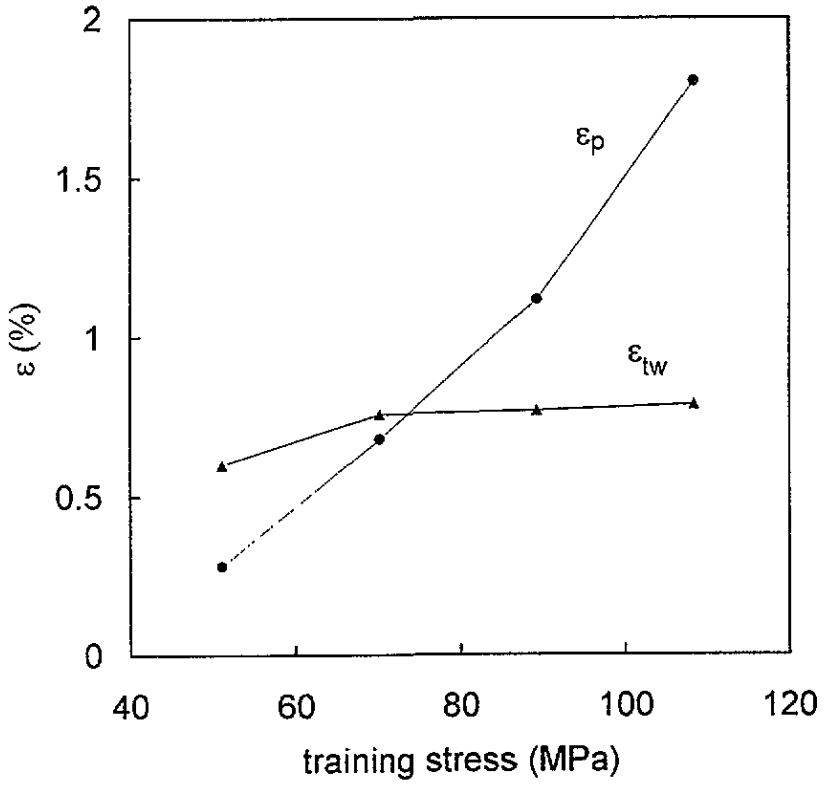

Figure 5. Two-way strain ε_{tw} (▲) and plastic strain ε_p (●) at the end of training, as functions of the training stress.

transformation for that purpose, as shown in the inset in figure 2.

From Ohm's law, $\Delta R/R_0$ in an isotropic conductor wire submitted to a total tensile strain ε is expected to follow the relation

$$\Delta R/R_0 = \Delta\rho/\rho_0 + (1 + 2\nu)\varepsilon \tag{1}$$

where ρ is the electrical resistivity and ν is Poisson's ratio. In conventional materials, in the elastic region, ν is constant and less than 0.5 while, in the plastic region, $\nu = 0.5$, as a consequence of the *plastic flow* condition, where the volume is invariant [11].

In a shape memory alloy submitted to a tensile stress, during a phase transition, the total strain ε is given by $\varepsilon = \varepsilon_{el} + \varepsilon_p + \varepsilon_{tr}$, where ε_{el} is the elastic strain, ε_p is the plastic strain and ε_{tr} is the transformation strain ($\varepsilon_{tr} = \varepsilon_{tw}$ in the stress-free condition). Poisson's ratios in the elastic region for B2 and B19′ phases were found in Ti–Ni single crystals to be 0.43 and 0.35, respectively [12]. The process of the detwinning characteristic of the selected growth of variants (and variant reorientation) is reasonably expected to be volume invariant, thus suggesting a constant value of 0.5 for ν, as in the plastic flow condition. Since $0.35 < \nu < 0.5$ and $\varepsilon_p + \varepsilon_{tr} > \varepsilon_{el}$, for a rough calculation of the geometrical contribution to $\Delta R/R_0$ in the present case the constant value of 0.5 has been used for ν.

4.1. B2 phase

In the B2 phase, equation (1) can be written as follows:

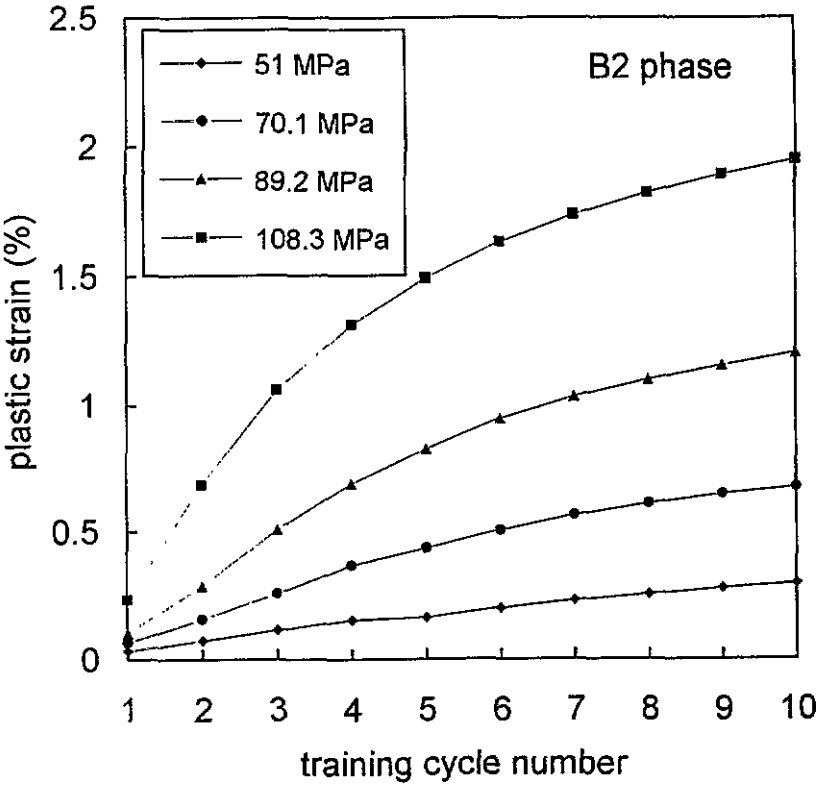

Figure 6. Plastic strain stored in the B2 phase as a function of the training cycle number, for each training stress level investigated.

$$\Delta R/R_0 = [\Delta\rho/\rho_0]_p + (1+2\nu)(\varepsilon_p + \varepsilon_{el}) \tag{2}$$

where $[\Delta\rho/\rho_0]_p$ is the resistivity due to the introduction of line defects, related to the plastic strain stored as a consequence of training. The analysis of $\Delta R/R_0$ versus ε_p data allows one to evaluate the $[\Delta\rho/\rho_0]_p$ term in (2). In fact, $(1+2\nu)\varepsilon_{el}$ is constant, and

$$\partial(\Delta R/R_0)/\partial\varepsilon_p = \partial[\Delta\rho/\rho_0]_p/\partial\varepsilon_p + (1+2\nu). \tag{3}$$

Experimental data show that $\Delta R/R_0$ versus ε_p follow a linear trend (see figure 7) with slopes of 2.64 at 51 MPa, 2.51 at 70.1 MPa, and 2.62 at 89.2 MPa. The good agreement between the results related to the three stress levels investigated suggests that the same deformation micromechanism is active. It can therefore be inferred that $[\Delta\rho/\rho_0]_p$ is linearly related to ε_p. Since the expected geometrical contribution $1+2\nu$ is 2, following equation (3) the higher value of about 2.6 found experimentally appears to be related to the resistivity contribution $[\Delta\rho/\rho_0]_p$. Equation (2) can be written as follows:

$$\Delta R/R_0 = \alpha\varepsilon_p + (1+2\nu)(\varepsilon_p + \varepsilon_{el})$$

where $\alpha \simeq 0.6$.

This does not apply to the results obained at the highest training stress of 108.3 MPa, which can be explained by the presence of some martensite not retransformed in the parent phase under applied stress [13, 14].

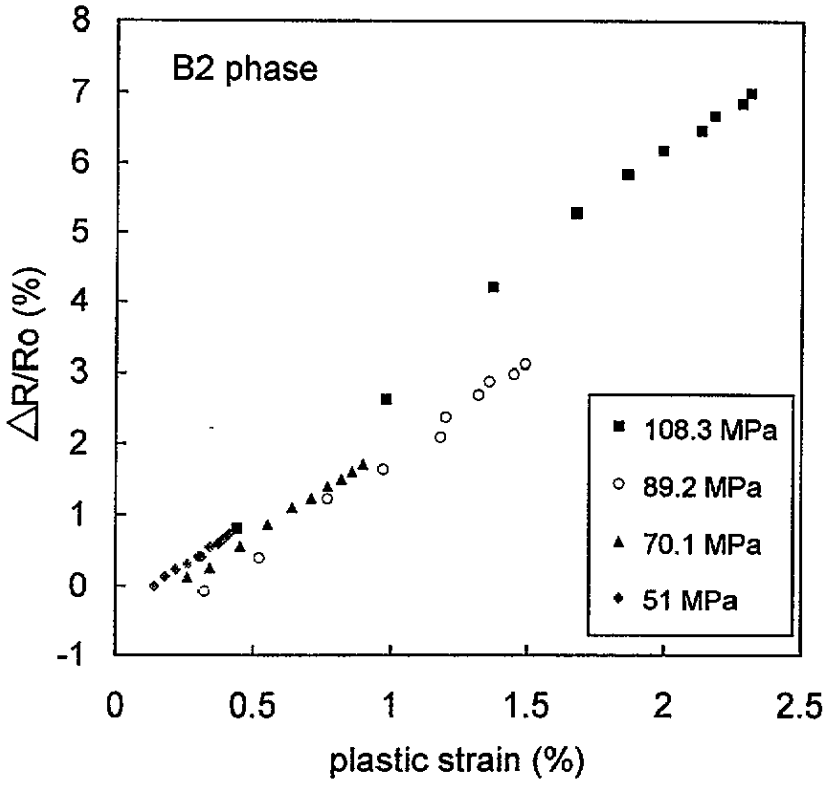

Figure 7. $\Delta R/R_0$ versus plastic strain stored in the B2 phase during the different training cycles, for each training stress level investigated.

4.2. B2 ↔ B19 transition

During the B2 ↔ B19 transition a linear relationship between $\Delta R/R_0$ and the total strain ε has also been found both on training, except for the first few cycles, and after training (see figures 8 and 9). The slope of $\Delta R/R_0$ versus ε was about 5.5 during training and slightly lower (about 5) during the TWME (figure 8). In the transformation range, $\Delta R/R_0$ depends on both strain and temperature and equation (1) can be written

$$\Delta R/R_0 = [\Delta\rho/\rho_0]_p + [\Delta\rho/\rho_0]_{var} + [\Delta\rho/\rho_0]_{th} + (1+2\nu)\varepsilon \tag{4}$$

where the following hold.

(i) $\varepsilon = \varepsilon_{el} + \varepsilon_p + \varepsilon_{tr}$ is the total strain.

(ii) $[\Delta\rho/\rho_0]_p = \alpha\varepsilon_p$ is the resistivity change due to the introduction of line defects, related to the plastic strain stored during training. As discussed above, $[\Delta\rho/\rho_0]_p$ is linear with ε_p.

(iii) $[\Delta\rho/\rho_0]_{var}$ is characteristic of shape memory alloys, where variant reorientation takes place under stress. During the variant reorientation process in martensite, at least at a constant temperature in Ti–Ni shape memory alloys, a linear trend has been found [15, 16]; this appears to be applicable also in the present case, where specific variants grow or shrink either under stress or in the stress-free condition during the TWME; hence $[\Delta\rho/\rho_0]_{var} = \beta\varepsilon_{tr}$.

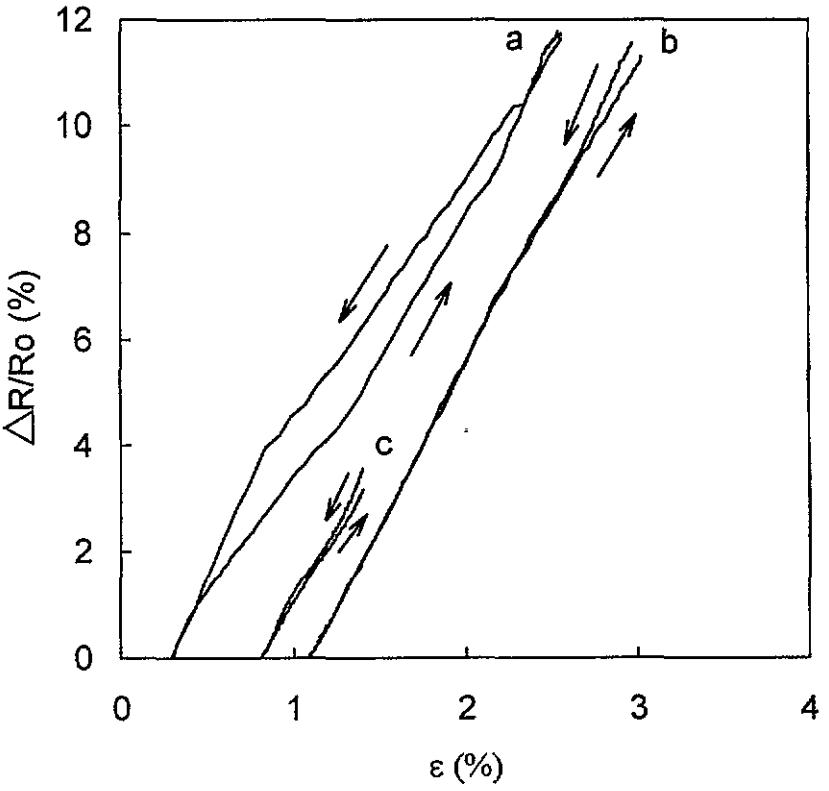

Figure 8. $\Delta R/R_0$ versus ε in the range of the B2 $\leftrightarrow$ B19 transformation (a) during the first training cycle at 70.1 MPa, (b) during the tenth training cycle at 70.1 MPa and (c) during the thermal cycle after training showing the TWME.

(iv) $[\Delta\rho/\rho_0]_{th}$, a function of T, is due to the resistivity temperature dependence of the two phases, which coexist in the transformation region; in the present case, this term gives a small opposite contribution with respect to the other contributions, as can be deduced in the inset of figure 2; as a linear relation between the transformation strain and the transformed phase fraction is reasonably expected, one can conclude that this contribution, although small, is linearly dependent upon ε_{tr}, allowing one to write $[\Delta\rho/\rho_0]_{th} = \gamma\varepsilon_{tr}$.

In the light of the above remarks, it is not surprising to find for $\Delta R/R_0$ a linear relation with ε in the temperature range of the B2 $\leftrightarrow$ B19 transformation, both on training and after training. Neglecting the $\gamma\varepsilon_{tr} = [\Delta\rho/\rho_0]_{th}$ contribution, from equation (4), one obtains for the slope

$$d(\Delta R/R_0)/d\varepsilon = \alpha + \beta + 1 + 2\nu.$$

Since a value of about 5.5 has been found for $\alpha + \beta + 1 + 2\nu$ and since $\alpha \simeq 0.6$, on the assumption that $\nu = 0.5$, then $\beta \simeq 2.9$. This result is slightly higher than found for Ti–Ni [15, 16]. The difference could derive from the different mechanisms of growth; in the present case a selected variant growth takes place under stress, while in Ti–Ni in martensite a reorientation of existing variants takes place.

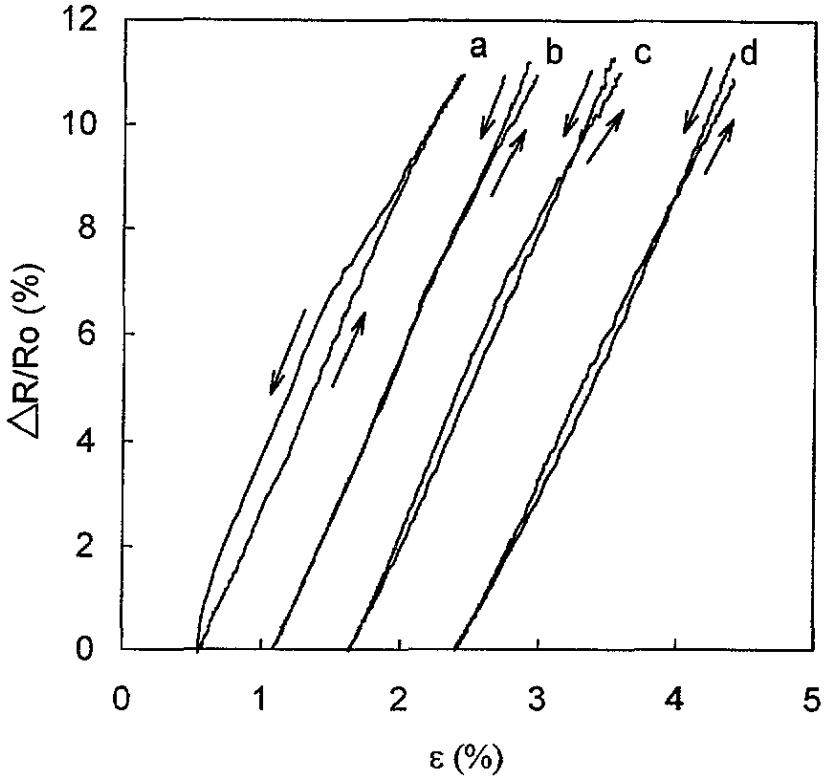

Figure 9. $\Delta R/R_0$ versus ε in the range of the B2 ↔ B19 transformation during the tenth training cycle at (a) 51 MPa, (b) 70.1 MPa, (c) 89.2 MPa and (d) 108.3 MPa stresses.

5. Conclusion

Training to imprint the TWME has been investigated here, involving the B2 ↔ B19 phase transformation in a 50 at.% Ti–40 at.% Ni–10 at.% Cu shape memory alloy. The ε_{tw} impressed is about 0.8%. The optimal training stress to obtain the TWME was 70.1 MPa; for higher stresses, significant increases in ε_{tw} were not achieved, whilst high levels of ε_p were accumulated.

Attention has been focused on the ER change during the B2 ↔ B19 transition. Evidence was given that $\Delta R/R_0$ versus ε follows a linear relationship with approximately the same slope during training and after training in the TWME; the result is relevant *per se* and furthermore looks appealing for application to the control of shape memory actuators.

The resistivity and geometrical contributions to the ER change have been examined.

(i) The electrical resistivity modification induced by the plastic strain stored as a consequence of training was found to be linear with ε_p at least for stresses lower than 90 MPa.

(ii) A contribution to the electrical resistivity change ascribed to a selected variant growth has been obtained, slightly higher than found for the detwinning process in martensitic Ti–Ni

A training stress of 70 MPa appeared as the most apt to imprint a TWME related to B2 ↔ B19 transformation and to obtain a linear relationship for $\Delta R/R_0$ versus ε in the same range.

Acknowledgments

The research has been supported by the Progetto Finalizzato Materiali Speciali per Tecnologie Avanzate del Consiglio Nazionale delle Ricerche. The specimens were kindly supplied by Furukawa Electric Co., Japan, here gratefully acknowledged.

References

[1] Schroeder T A and Wayman C M 1977 *Scr. Metall.* **11** 250
[2] Liu Y and McCormick P G 1988 *Scr. Metall.* **22** 1327
[3] Liu Y and McCormick P G 1990 *Acta Metall. Mater.* **38** 1321
[4] Perkins J and Sponholz R O 1984 *Metall. Trans.* A **15** 313
[5] Stalmans R, Van Humbeeck J and Delaey L 1992 *Acta Metall. Mater.* **40** 2921
[6] Nam T H, Saburi T, Kawamura Y and Shimizu K 1991 *Mater. Trans. Japan Inst. Met.* **31** 262
[7] Nam T H, Saburi T and Shimizu K 1990 *Mater. Trans. Japan Inst. Met.* **31** 959
[8] Lo Y C, Wu S K and Horng H E 1993 *Acta Metall. Mater.* **41** 747
[9] Miyazaki S, Shiota I, Otsuka K and Tamura H 1989 *Proc. Int. Meet. on Advanced Materials* vol 9 (Pittsburgh, PA: Materials Research Society) p 153
[10] Airoldi G, Ranucci T, Riva G and Sciacca A 1995 *Scr. Metall.* submitted for publication
[11] Gere G M and Timoshenko S P 1990 *Mechanics of Materials*, Thomson Formation Publishing Group (Boston, MA: PWS Kent) p 26
[12] Brill M T, Mittelbach S, Assmust W, Moellner M and Loethi B 1991 *J. Phys.: Condens. Matter* **3** 9621
[13] Airoldi G, Ranucci T and Riva G 1994 *Trans. Mater. Res. Soc. Japan* B **18** 1109
[14] Stalmans R, Van Humbeeck J and Delaey L 1992 *Acta Metall. Mater.* **40** 501
[15] Airoldi G, Ranucci T and Riva G 1991 *J. Physique* C **4** (Supplement III) 439
[16] Airoldi G, Ranucci T, Riva G and Vicentini B 1992 *Shape Memory Materials and Phenomena—Fundamental Aspects and Application (3–5 December, 1991, Boston, MA) (Mater Res. Soc. Symp. Proc. 246)* (Pittsburgh, PA: Materials Research Society) p 277